International Symposium
On Turbulence and Shear Flow
Phenomena (TSFP-9)
June 30 - July 3, 2015 *Melbourne, Australia*

Rapid growth of unsteady finite-amplitude perturbations in a supersonic boundary-layer flow

Daisuke Watanabe
Graduate School of Engineering
Toyama University
3190 Gofuku, Toyama-shi, Toyama 930-8555, Japan
dwata@eng.u-toyama.ac.jp

Hiroshi Maekawa
Graduate School of Informatics and Engineering
The University of electro-communications
1-5-1 Chofugaoka, Chofu-shi, Tokyo 182-8585, Japan
maekawa@mce.uec.ac.jp

ABSTRACT

Spatial numerical simulations (SNS) are performed to study transition to turbulence in a supersonic flat plate boundary layer forced by finite amplitude perturbations, where the freestream Mach numbers is 2.5 with the isothermal wall condition. Three-dimensional isotropic disturbances are superimposed on the laminar profile for Reynolds number based on the displacement thickness $\delta^*$of 1000 at the inlet plane of the computational domain. The effects of the peak location of the disturbance spectrum and the magnitude distribution in the wall normal direction are analyzed. Numerical results indicate that energy spectra with a peak located at around the wavenumber of k_{max}=1.0 play an important role to induce transition to turbulence. The disturbance at lower wavenumbers with concomitant turbulence in the free stream shows an early appearance of hairpin-like structure in the transition region. The vortical structures on set of transition to turbulence rapid evolving to a hairpin packet with fine secondary structures downstream are shown in this paper, which is an inherent structure induces transition to turbulence in the supersonic boundary layer.

INTRODUCTION

A deep understanding of the principal route to turbulence in the wall-bounded shear flows is of great fundamental and practical interest. Various disturbances affect transition to turbulence in a laminar boundary layer, which has been investigated in detail so far. The primary stage of transition in a low-turbulence environment has been extensively studied by stability theories (Mack 1975) and flow fluctuation measurements by Kendall (1975) or Graziousi & Brown (2002). Understanding of the late stage of transition scenario or the nonlinear transition (Graziousi & Brown 2002) due to high level disturbances for boundary layers is even less pronounced especially for supersonic one due to experimental difficulties.

In this study, a spatial simulation of a supersonic, isothermal flat plate boundary layer flow at Mach 2.5 is analyzed. Growth of finite amplitude disturbances on transition to turbulence in a developing boundary layer downstream require the application of fully spatial formation in a numerical simulation without extended temporal simplifying assumptions. The emphasis of this study is to assess the transitional scenarios for supersonic boundary layer and the late stage of streak breakdown and observing the transitional structures in a Lagrangian tracking manner, which leads to finding an inherent structure generated from finite-amplitude perturbations which induces transition to turbulence in the supersonic boundary layer.

SMULATION DETAILS

In the SNS of spatially developing boundary layer, the non-dimensional equations governing the conservation of mass, momentum, and energy for a compressible Newtonian fluid are solved. Note that displacement thickness at the inlet boundary layer (δ^*) is chosen to be a representative length scale.

The computational domain size is $L_x \times L_y \times L_z = 300\delta^* \times 30\delta^* \times 33\delta^*$. The form of the solenoidal disturbance is given as

$$E(k) = k^4 \exp\left[-2(k/k_{max})^2\right], \qquad (1)$$

where k is wavenumber and the turbulence energy peak locates at k_{max}. In order to meet the no-slip boundary condition at a wall, a window function to impose zero velocities at the wall is used. High-order compact upwind biased scheme with boundary schemes (Deng et al. 1996, Deng & Maekawa 1997) are used for spatial derivatives and a 4th-order Runge-Kutta scheme for time advancement. The Navier-Stokes characteristic boundary conditions by Poinsot and Lele (1992) are used in the streamwise and normal directions and periodic boundary conditions in the spanwise direction. For 3-D spatial numerical simulations, after a grid-convergence analysis,

the computational grid is $N_x \times N_y \times N_z$ = 901×101×96. The grid is clustered toward the wall in the wall normal direction. The finite amplitude of the disturbance is 1, 1.5, 2, 2.5% at the boundary layer inlet and k_{max} is 1.0 where the corresponding wavelength is $2\pi\delta^*$.

Note that a window width affects transition to turbulence in the cases of 1.5, 2, and 2.5%. Figure 1 shows the window widths employed in this simulation, where the inlet streamwise velocity distribution is also presented.

In the preliminary simulations of various disturbances, the effect of k_{max} was investigated, where the employed k_{max} of the disturbances are π, 2.0, 1.0 and 0.5 and the magnitude of each disturbance is 2.0%.

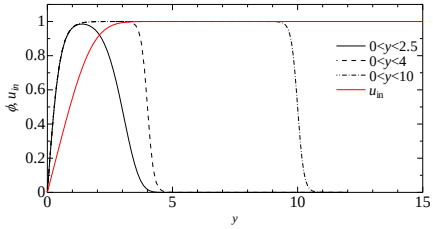

Fig. 1 The distributions of the window functions ϕ and the inlet mean streamwise velocity u_{in} presented by red line.

RESULTS

First of all, the effect of k_{max} was investigated. Figure 2 shows a top view of the visualized low-speed streaks (blue contours) and quasi-streamwise vortices with hairpin packets (yellow contours).

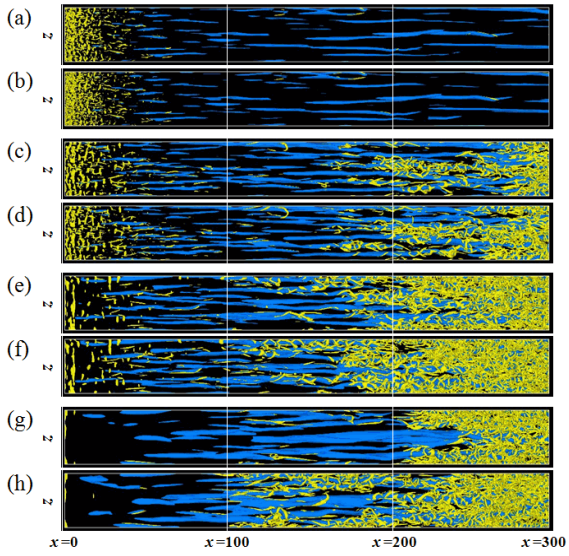

Fig. 2 Downstream evolution of second invariant Q(=0.005; yellow) structure and low-speed streak u'(= -0.1; blue) for 2.0% case; a) k_{max} =π, y<4, b) k_{max}=π, y<10, c) k_{max} =2.0, y<4, d) k_{max} =2.0, y<10,e) k_{max} =1.0, y<4, f) k_{max} =1.0, y<10, g) k_{max}=0.5,y<4 and h) k_{max}=0.5, y<10.

A comparison between Fig.2 (a), (c), (e), and (g) indicates the effect of k_{max} of the disturbance on the transitional structure in the boundary layer, when the flow is forced by the disturbance with the same window width of 0<y<4, as shown in Fig.1. Figures 2 (b), (d), (f), and (h) also show the effects of k_{max} of the disturbance on the transitional structure in the boundary layer, where the same window of 0<y<10 is adopted.

Figure 2 shows the long streamwise low-speed streaks shown by blue contours with a wall plane. As shown in Fig. 2 (a) and (b), low-speed regions are associated quasi-streamwise near-wall vortices. Quasi-streamwise vortices appear on the flank of the streak. Figures 3 (c), (d), (e), (f), (g) and (h) show many arch-vortices and these quasi-streamwise vortices as well. Isolated near-wall arch structures are clearly visualized in Fig.2(c) and (d). Successive arch structures or hairpin heads on the low-speed streak are dominant at downstream locations of x>100 in Figs.2 (e), (f), (g) and (h). These numerical results indicate that transition is induced effectively by forcing at the lower wavenumbers of k_{max} such as kmax=1.0 and 0.5 with the wide windows of 0<y<10. A comparison of Fig.2 (g) and (h) indicates that forcing with wide windows is effective to create successive hairpins. Figure 3 indicates the evolution of the shape-factor of the boundary layer forced by various upstream disturbances with three window widths of y<2.5, y<4, and y<10, where the magnitude of each disturbance is 2.0%.

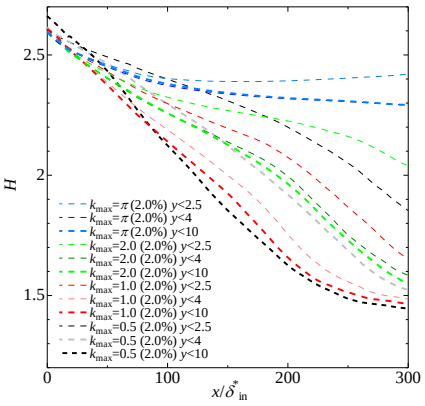

Fig. 3 Downstream evolution of shape factor for the disturbance magnitude of 2.0%.

Figures 4 and 5 show the Fourier spectrum of u velocity fluctuation at the streamwise location of x/δ^*=150 (mid-plane in the streamwise direction) for the flow forced by the disturbance of k_{max}=2.0 and 1.0, respectively, where β indicates spanwise wave number. As Fig. 4 shows, the spectrum peak locates at β =1.0 corresponding to the streaky structures in the instantaneous flow field. As shown in Fig.2(c), isolated arches appears around x/δ^*=150. On the other hand, as shown in Fig.2 (e), successive hairpins appear around x=150. A comparison of Fig.4 and Fig.5 indicate that streaky structures with the isolated arch on the low-speed streak are dominant at x=150, however successive hairpins appears in Fig.5,

where Fourier spectrum at $0.5<\beta<2.0$ becomes dominant in this transitional flow. In the turbulent boundary layer downstream, by the formation of an arch vortex (arch of horseshoe) spanning a few streaks, the elongated streak disappears. The upstream lift-up streak and adjacent streaks create another hairpin packets (secondary and tertiary hairpins), after a short evolution, these trailing legs fill the boundary layer inside.

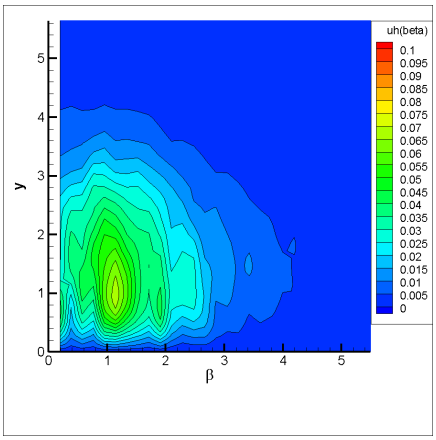

Figure 4. Fourier spectrum of velocity fluctuation in the case of k_{max} =2.0 and the width of window function of $0<y<4\delta^*$(x/ δ^*=150) .

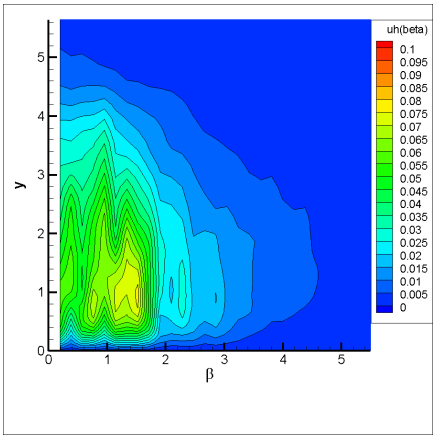

Figure 5. Fourier spectrum of velocity fluctuation in the case of k_{max} = 1.0 and the width of window function of $0<y<4\delta^*$(x/ δ^*=150).

As indicated in the evolution of the shape-factor of the boundary layer shown in Fig.3, forcing by the disturbances at the lower wavenumbers of k_{max} such as k_{max} =1.0 and 0.5 with the wide windows of $0<y<10$ is effective for transition to turbulence. Secondly, in this paper, effects of the magnitude of the disturbance are investigated for the disturbance of k_{max} =1.0, which is of effective to induce transition and no essential difference is observed in the transitional flow forced by the disturbance k_{max} =0.5, as shown in Fig.3, where the decaying shape-factor in the cases of k_{max} =1.0 and 0.5 are similar.

Figure 6 indicates the evolution of the shape-factor of the boundary layer forced by various upstream disturbances, where k_{max} is 1.0, the disturbance magnitudes are 1, 1.5, 2, 2.5% of the freestream velocity and the widths of the window function are $0<y<2.5\delta^*$, $0<y<4\delta^*$, $0<y<10\delta^*$. When the magnitude is very small at the present Reynolds and Mach numbers, transition to turbulence is not achieved in the simulation, different paths to transition may be active (see Fedorov (2011)). However, the magnitude of this disturbance is more than 1.0% seems to leads transition to turbulence.

COHERENT MINIMAL STRUCTURE

In this section, we will focus our attention on the slower transitional structures in the computational domain of $0<x/\delta^*<300$. For instances, the flow forced by the disturbance of the magnitude of 2% with all of the window width, and the flow forced by the disturbance of the magnitude is 1.5% with the window width of $0<y<10$ or $0<y<4$ are focused in this section.

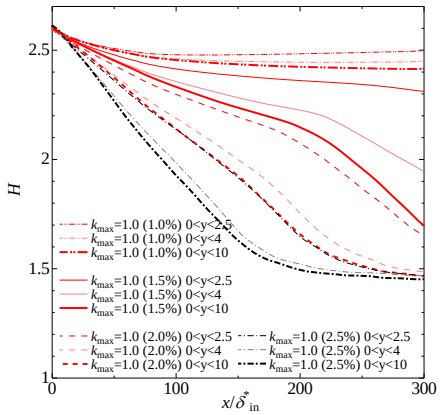

Figure 6. Evolution of shape-factor of the boundary layer forced by various upstream disturbances (Parameters are magnitude of disturbance and width of the window function)

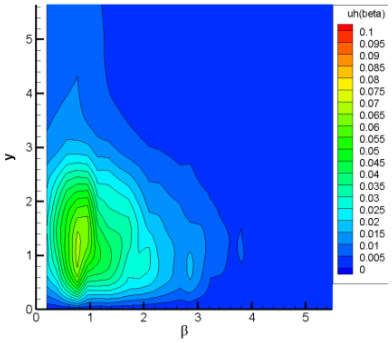

Figure 7. Fourier spectrum of velocity fluctuation in the case of the magnitude of 2% and the width of window function of $0<y<10\delta^*$.

Figure 7 shows the Fourier spectrum of u velocity fluctuation, where β indicates spanwise wave number. As this figure shows, the spectrum peak locates at β =0.8～1.0 corresponding to the streaky structures appeared in the instantaneous flow field. In these cases, we can find a few typical structure and streaky structures as well, where these structures grow or develop quickly downstream and these structures are usually localized or isolated in the flow field.

Duguet et al. (2012) performed direct numerical simulations of the low-speed boundary layer to track the dynamics in the region of phase space separating transitional from relaminarizing trajectories. They found that the structure is dominated by a robust pair of low-speed streaks, whose instabilities generate hairpin vortices evolving downstream into transient disturbances. Cherbini et al. (2013) showed localized flow structures living on the edge of chaos to understand transition to turbulence. They defined the structure as the hairpin-dominated edge state. Recent progress in understanding transition to turbulence is based on the application of concepts from dynamical systems theory. The picture that emerges builds on invariant solutions of the Navier-Stokes equations such as fixed points and traveling waves.

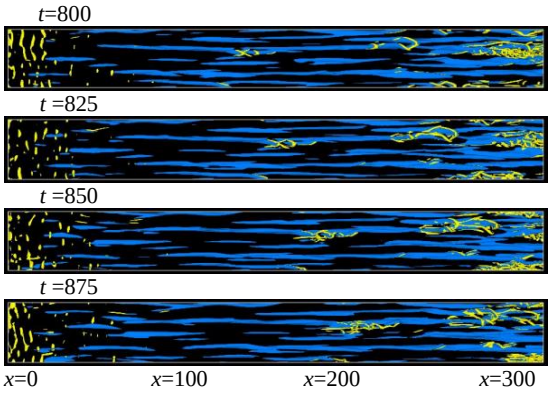

Figure 8. Snapshots of the vortical structure structure emerged at the downstream location around x=120 at nondimensional time t=800. The magnitude of disturbance is 2% of the freestream velocity and the window width is $0<y<2.5\delta^*$.

Figure 8 shows the visualized low-speed streaks (color: blue, isosurface of u=-0.1) and the vortical structures (color: yellow, isosurface of Q=0.005) visualized with iso-surfaces of the second invariant Q of the velocity gradient tensor evolving to a hairpin packet at the non-dimensional time respectively. The visualized vortical structures on set of transition to turbulence are observed, where spanwise-inclined vortices and hairpin heads appear around $x=120\delta^*$ at t=800 and fine structures evolve along the streak shown in successive snapshots at t=825, 850 and 875. Another onset structures are observed around $x=220\delta^*$ at t=800. Hairpin heads observing in the outer boundary layer are due to the lift-up low-speed streaks (see Cherubini et al. b 2011). This fact suggests that an inherent structure induces transition to turbulence in the boundary layer. Cherubini et al. investigated the linear and nonlinear optimal perturbations in a low-speed boundary layer. The nonlinear optimal is characterized by spanwise inclined vortices, whereas the linear optimal contains streamwise vortices.

Another evidence of evolution to turbulent boundary layer is energy spectrum at various stages. Energy spectrum indicates the statistical feature of the transitional stages.

Figures 9 a) and b) indicate the energy spectra of fluctuating u velocities at $x=60\delta^*$ and $120\delta^*$, where St is Strouhal number defined by the displacement thickness and the freestream velocity. The Strouhal number indicates the corresponding wave number and non-dimensional frequency. As these figures show, the peak at St=0.1 appears at $y=0.5\delta^*$ (Black line) in the case at $x=60\delta^*$, then the rapid growth in the spectrum downstream. Note that the sampling frequency used for time averaging is not high enough to capture high frequency phenomena in the simulation. Therefore, the energy spectrum employed for time averaging to obtain longer time data series does not follow high frequency phenomena, as shown in Fig.9 (b). The energy shows no decrease for higher wavenumbers.

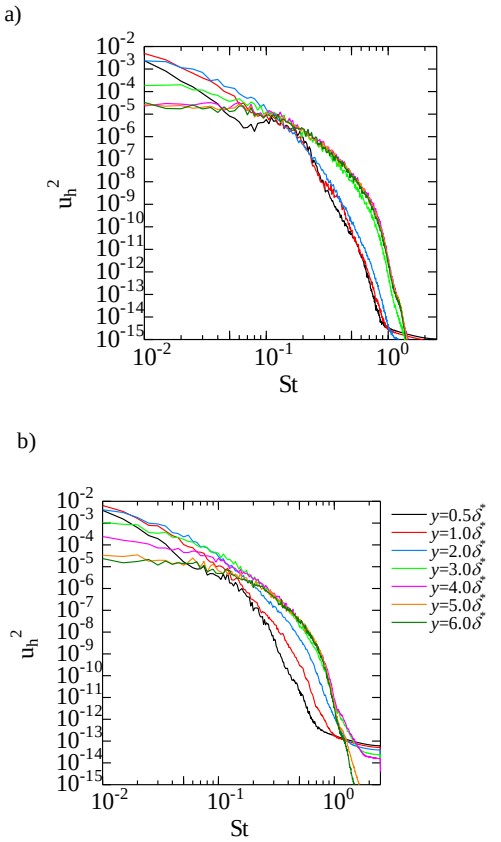

Figure 9. Energy spectra of u velocity fluctuations for a) $x=60\delta^*$, b) $x=120\delta^*$. The magnitude of disturbance is 2% and the window width is $0<y<10\delta^*$.

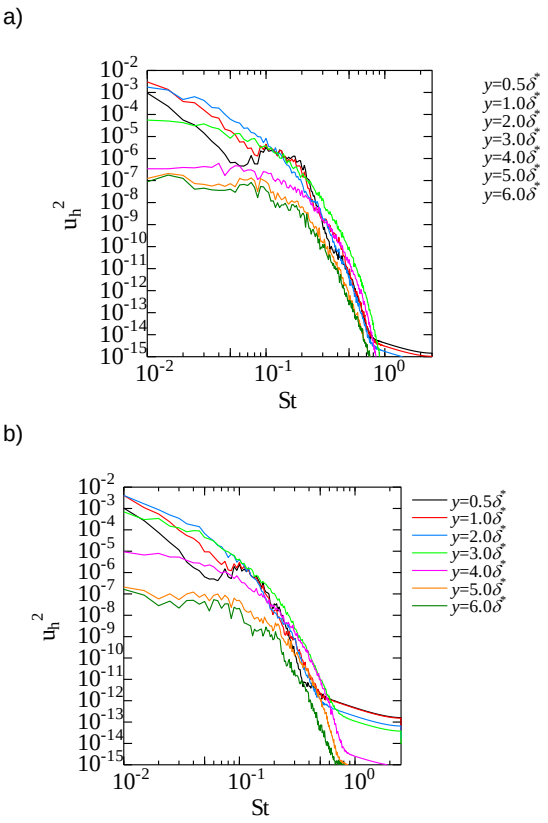

Figure 10. Energy spectra of u velocity fluctuations for a) $x=60\delta^*$, b) $x=120\delta^*$. The magnitude of disturbance is 2% and the window width is $0<y<2.5\delta^*$.

The instantaneous flow field shows that the fine structures appear downstream and the oscillatory and breakdown of the low-speed streaks can be observed in the cases of high magnitude and the low magnitude with wide width of window function. However, as shown in Fig.2, in the case of the window function of $0<y<2.5\delta^*$, the energy spectrum grows gradually. Figure 10 shows the energy spectra of fluctuating u velocities at $x=60\delta^*$ and $120\delta^*$ of the flow field forced with the window function of $0<y<2.5\delta^*$. As Fig.10 (b) shows, the bump peak at $St=0.1$ at $y=0.5\delta^*$ still appears at $x=120\delta^*$, which corresponds to the slower evolving of isolated spanwise-inclined vortices with a hairpin. This fact suggests that there is a minimal characteristic structure generated from the finite amplitude perturbations that induces transition to turbulence. Hairpin-shaped vortices found by Duguet et al. (2012) forms above the region where streaks pinch. Optimal varicose perturbations grows very rapidly in a boundary layer. Such optimal disturbances lead to transition for initial energies. The structure found in this supersonic boundary layer simulation is close to hairpin vortices on pinched streaks in incompressible boundary layers or the nonlinear optimum stage found by Cherubini et al. (2013).

On the contrary, as shown in Fig. 2 (e), the wider window of 0<y<4 brings a few successive hairpins on the streaky structure, which is important for rapid evolving into structure breakdown.

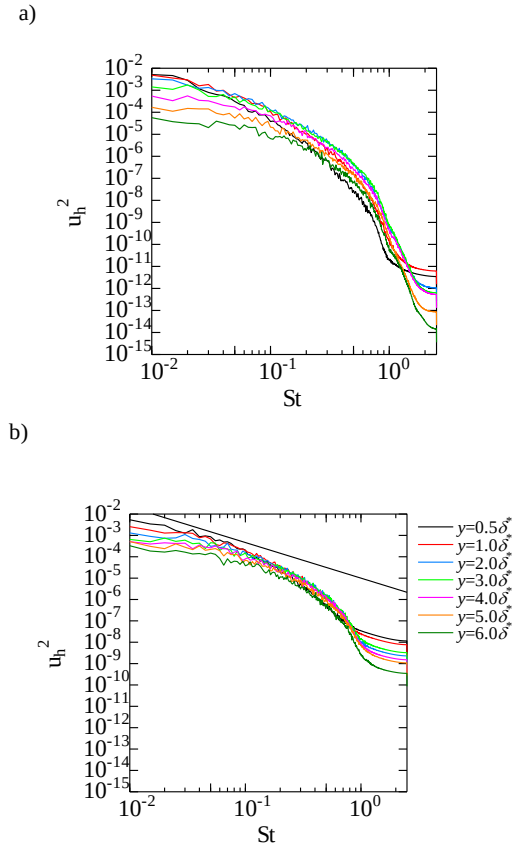

Figure 11. Energy spectra of u velocity fluctuations for a) $x=180\delta^*$, b) $x=270\delta^*$. The magnitude of disturbance is 2% and the window width is $0<y<10\delta^*$.

Figure 11 shows the energy spectra at $x=180\delta^*$ and $270\delta^*$. The shape-factors of the velocity profile at $x=180\delta^*$ and $270\delta^*$ and are higher and lower values than 1.5, respectively. As shown in Fig.11, where the straight line presents the power spectrum of -5/3, the energy is distributed in a cascade fashion at $x= 270\delta^*$.

SUMMARY

In this paper we present a few coherent minimal structures rapid evolving to a hairpin packet with fine secondary structures downstream, which is an inherent structure and induces transition to turbulence in the boundary layer. The structure is characterized spanwize-inclined vortices and successive hairpins on the low-speed streak. Energy spectrum indicates the statistical feature of the transitional stages generated by the coherent structure. The spanwise wave number peak locates at $\beta=1.0$, where the corresponding wavelength is $2\pi\delta^*$. The Strouhal number defined by the displacement thickness and the freestream velocity indicates the corresponding wave

number and non-dimensional frequency at St=0.1 inside the boundary layer.

ACKNOWLEDGEMENTS

This study was partly supported by Grants-in-Aid for scientific research (21560165, 24656518) from Japanese Ministry of Education, Culture, Sports, Science and Technology.

REFERENCES

Cherubini S., De Palma P. and Robinet J.-C., 2011a, The minimal seed of turbulence transition in a boundary layer flow *J. Fluid Mech.* Vol.689, pp.221-253.

Cherubini S., De Palma P. and Robinet J.-C. and Bottaro A., 2011b, Edge states in a boundary layer, *Physics in Fluids*, Vol.23, 051705.

Cherubini S., De Tullio M. D., De Palma P. and Pascazio G., 2013, Transient growth of the flow past a three-dimensional smooth roughness element, *J. Fluid Mech.* Vol.724, pp.642-670.

Deng, X., Maekawa, H. and Shen, C., 1996, A Class of High Order Dissipative Compact Schemes, *AIAA Paper*, No. 96-1972.

Deng X. and Maekawa H., 1997, Compact high-order accurate nonlinear schemes. *Journal of Computational Physics,* Vol. 130, pp. 77-91.

Duguet Y., Schlatter P., Henningson D. S., Eckhardt B., 2012, Self-Sustained Localized Structures in a Boundary Layer Flow, *Physical Review Letters,* Vol.108, 044501.

Fedorov A., 2011, Transition and Stability of High-Speed Boundary Layers *Annu. Rev. Fluid Mech.* Vol 43, pp.79-95.

Graziousi,P.& Brown G., 2002, Experiments on stability and transition at Mach 3, *J. Fluid Mech.*,Vol.407, pp.83-124.

Kendall, J.M., 1975, Wind Tunnel Experiments Relating to Supersonic and Hypersonic Boundary layer Transition, *AIAA J.* Vol.13, pp.290-299.

Poinsot T J and Lele S K, 1992, Boundary Conditions for Direct Simulations of Compressible Viscous Flows, *Journal Computational Physics,* Vol.101, pp.104-129.